energies

MDPI

Article

Research on Neutronics Safety Parameters of the AP1000 Nuclear Reactor under Different Conditions

Xinyi Niu, Jianquan Liu *, Zenghao Dong, Jie Wei and Wenlong Zhou

College of Energy and Mechanical Engineering, Shanghai University of Electric Power, Shanghai 201306, China
* Correspondence: liujianquan@shiep.edu.cn

Abstract: Changes in temperature during reactor operation may cause changes in physical parameters, leading to core overheating and accidents. It is essential to analyze and assess the safety parameters of the core under different operating conditions. This paper investigates the effects of fuel temperature, moderator density, boron concentration, and control rod state on AP1000 safety parameters. The study uses RMC and NJOY to calculate the changes in reactivity factor, effective delayed neutron fraction, and neutron generation time of the AP1000 reactor under different operating conditions. The changes in reactivity coefficients, neutron fluxes, and relative power densities of AP1000 reactors are analyzed for normal and accidental operating conditions. The results indicated that the reactivity coefficient remained negative under accident conditions, which ensured the safe operation of the reactor. The delayed neutron fraction, neutron flux, and power density distributions are affected by fuel temperature, moderator density, and control rod position. The control rod worth was sufficient for the emergency shutdown of the reactor under accidental conditions. It is demonstrated that the operation of the AP1000 reactor under study conditions is safe and controllable.

Keywords: AP1000; Monte Carlo; safety parameters; accident conditions

check for updates

Citation: Niu, X.; Liu, J.; Dong, Z.; Wei, J.; Zhou, W. Research on Neutronics Safety Parameters of the AP1000 Nuclear Reactor under Different Conditions. *Energies* **2023**, *16*, 7549. https://doi.org/10.3390/en16227549

Academic Editor: Chunyan Zou

Received: 13 October 2023
Revised: 2 November 2023
Accepted: 7 November 2023
Published: 13 November 2023

1. Introduction

The reactor is the core equipment of a nuclear power plant. According to the different moderators and coolants, reactors can be categorized into water-cooled reactors, gas-cooled reactors, liquid metal-cooled reactors, and molten salt reactors. Water-cooled reactors are further categorized into light water reactors (LWR) and Heavy Water Reactors (HWR). Pressurized water reactors (PWR) are light water reactors among water-cooled reactors. The current representative reactor type among gas-cooled reactors is the Modular High-Temperature Gas-Cooled Reactor [1]. The most mature and representative type of liquid metal-cooled reactor is the sodium-cooled fast reactor. Pressurized water reactors (PWR) are the main type of reactors used in operating nuclear power plants around the world.

During start-up, operation, and shutdown of the reactor, the physical parameters and reactivity of the core are constantly changing. Changes in core temperature affect some physical parameters within the reactor. For example, an increase in fuel temperature leads to a broadening of the resonance absorption peaks in the fuel target nucleus, an increase in the resonance absorption of neutrons, and a change in the neutron properties within the core, which is also known as the Doppler effect. Temperature changes also affect the solubility of soluble boron in the coolant and the density of the moderator. These influences will change the neutron balance within the core, causing changes in the effective multiplication factor (K_{eff}), thus causing changes in reactivity. Reactor core calculations are typically conducted using the Monte Carlo method. For instance, researchers have validated the reliability of the Monte Carlo software MBC by measuring and concentrating actinides and gadolinium isotopes in spent nuclear fuel from the Ohi-2 PWR [2,3]. In this paper, the Monte Carlo software RMC3.5 is used.

The reactor temperature coefficient is required to be negative in reactor design to ensure safe reactor operation. Researchers have calculated negative temperature reactivity coefficients to demonstrate that new reactors are inherently safe [4,5]. The AP1000, as an advanced pressurized water reactor developed with existing operating regimes, always has a negative temperature reactivity factor to maintain its inherent safety. By using different particle transport software, there have been a large number of studies on the calculation of temperature reactivity coefficients for different states of the AP1000 reactor core. Researchers have calculated the temperature effects in HFP, HZP, and CZP states by using NODAL3 and SRAC software, Serpent, and MCNP software [6–8]. Another scholar studied the Doppler effect of fuels at different temperatures [7–11]. However, most of the previous studies do not take into account the positive and negative reactivity coefficients of AP1000 cores at high temperatures. In this paper, the temperature reactivity coefficient at high temperatures is investigated to assess the safety of the reactor at high temperatures.

In addition, to ensure the safety of the reactor, reactivity needs to be controlled. Currently, in pressurized water reactors, reactivity is controlled by a combination of three control methods: control rods, solid combustibles, and the addition of boric acid solution to the coolant. The control rod worth and the boron worth are used to assess the reactor's ability to regulate. A large number of studies are presently used to calculate the control rod worth and the induced power changes [12–14]. Control rod worth calculations can be used to specify safety margins for reactors. For slow-changing reactivity, it depends on boric acid concentration compensated modulation. Some researchers have simulated and calculated the relationship between the boron worth and the burnup of the AP1000 core [15]. To further investigate the worth of reactor control rods and boric acid, the authors simulated the AP1000 control rod state and the working condition without boric acid. The reactivity control capability of AP1000 is explored.

The delayed neutrons are a crucial reactor safety parameter affecting the study of reactor transients [16,17]. The delayed neutron can maintain the critical controllability of the reactor. Currently, a large quantity of studies are devoted to the calculation of the effective delayed neutron fraction and uncertainty [18–20]. This is because nuclear reactor dynamics are largely influenced by the proportion of delayed neutrons in the total number of neutrons per fission. Since the effect of delayed neutrons on neutron lifetime is not negligible, they are usually studied together. However, the effect of delayed neutrons in the core as influenced by temperature and boron concentration is difficult to determine.

In conclusion, the temperature coefficients, delayed neutron fraction, and flux states of AP1000 cores are still not sufficiently investigated in the case of the high-temperature overheating of the reactor core. In this paper, the AP1000 reactor is selected as the research objective. The safety parameters of AP1000 in different states at wide temperatures are analyzed. The paper studies the reactivity coefficients of the reactor, such as fuel temperature coefficient (FTC), moderator density coefficient (MDC) at different temperatures, different locations of control rods, and different boron concentrations. The paper also studies the control of reactivity factors such as boron concentration coefficient (BCC) and control rod worth (CRW). The study calculates the accident safety performance of the AP1000 core. In addition, the effect of reactivity factors on the delayed neutron generation and average neutron generation time [12,16] is investigated. The effect of core overheating on neutron energy spectrum and power distribution is further calculated. The evaluation study of these parameters, especially the reactivity characterization of AP1000 at high temperatures, is important for the safe operation of AP1000 and other reactors.

2. Core Description and Calculation Methods

2.1. AP1000 Reactor Core Description

The AP1000 pressurized water reactor has a thermal power of 3400 MW. The core consists of 157 fuel assemblies arranged in a 17 × 17 elongated fuel assemblies arrangement [21]. The AP1000 reactor core is loaded with three fuel assemblies at different enrichment levels staggered in a tessellated pattern, as shown in Figure 1.

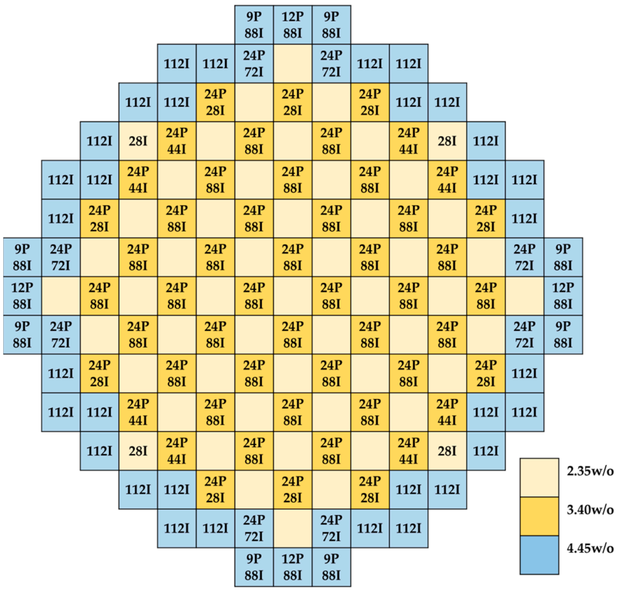

Figure 1. AP1000 reactor core showing the 3 regions of different ^{235}U enrichments.

The numbers indicate the amounts of burnable absorber rods of each type in a given fuel assembly: IFBA (I) and Pyrex (P). Each assembly has 289 positions, of which 264 positions are occupied by fuel elements and 24 positions are occupied by guide tubes to provide positions for the core functional assemblies. The guide tubes, together with the centrally located neutron measurement tubes and eight positioning grids along the height direction, form the skeleton of the fuel assembly to provide support. Figure 2 shows the RMC model of the fuel assembly without the core functional assembly and with control rods. In addition, Appendix A shows the 9 fuel assemblies in the AP1000.Details of the A1000 fuel assembly are shown in Table 1 [22]. The center of the single fuel rod is a low-enrichment-sintered UO2 ceramic core block, externally filled with helium and encapsulated in a zirconium–niobium alloy cladding.

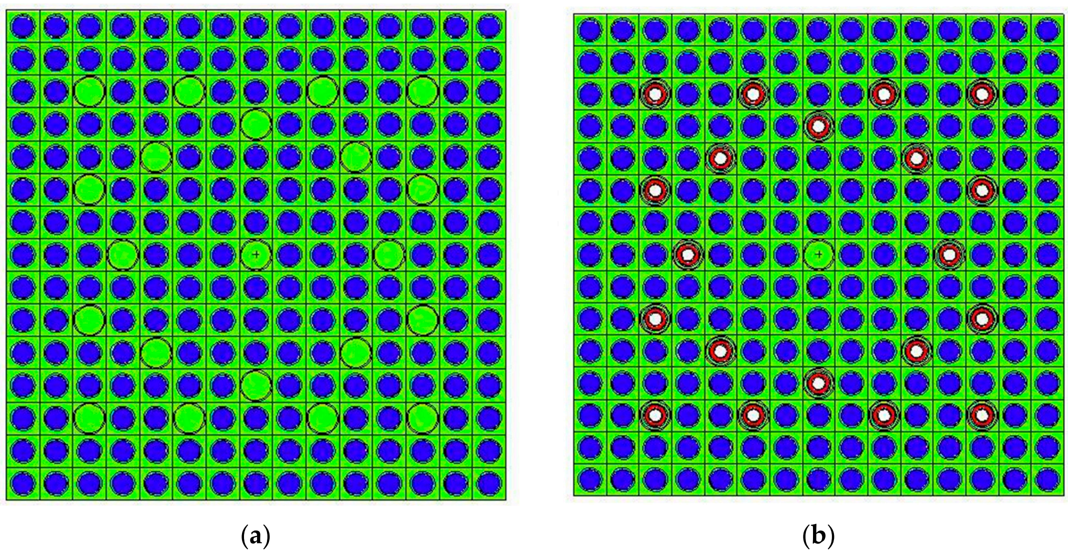

Figure 2. (**a**) Fuel assembly without control rods; (**b**) fuel assembly with control rods.

The burnable poison rods are primarily used for the first loading of the core, insertion into the fuel assembly, and occupying the fuel rods. The AP1000 uses separated burnable poison rods, known as Wet Annular Burnable Absorbent (WABA) [23]. It is used to suppress the initial excess reactivity of the core at the start of the cycle and to reduce the

RTC. Figure 1 shows the number of the Integral Fuel Burnable Absorber (IFBA) and the Pyrex Burnable Absorber.

Table 1. Details of AP1000 fuel assemblies.

Number of the fuel assembly	157
Fuel rods arrangement	17×17
Number of fuel rods in each assembly	264
Fuel rods pitch (cm)	1.26
Total fuel mass (kg)	0.214×0.214
Mass of zirconium alloy cladding (kg)	96,084
Number of grids in each assembly	14

The control rods are used to regulate the reactivity of the reactor during operation or for fast shutdown in emergencies. According to the purpose of control rods, control rods are categorized into regulating rods and shutdown rods. There are four sets of shutdown rods (SD) [24,25], each with eight bundles of control rod assemblies for rapid shutdown. There is only one set of Axial Offset Rods (AO) [24,25], consisting of nine bundles of control rod assemblies for axial power distribution control. There are six sets of Shim Rods (M) [24,25], which are used to compensate for daily reactivity changes. Figure 3 shows the distribution of control rods in the 1/4 core. There are 69 control rods in the AP1000 core. Reactor startup, shutdown, and fuel consumption compensation all require regulation of boron concentrations. Material and geometry data describing the AP1000 core are taken from the existing literature [26].

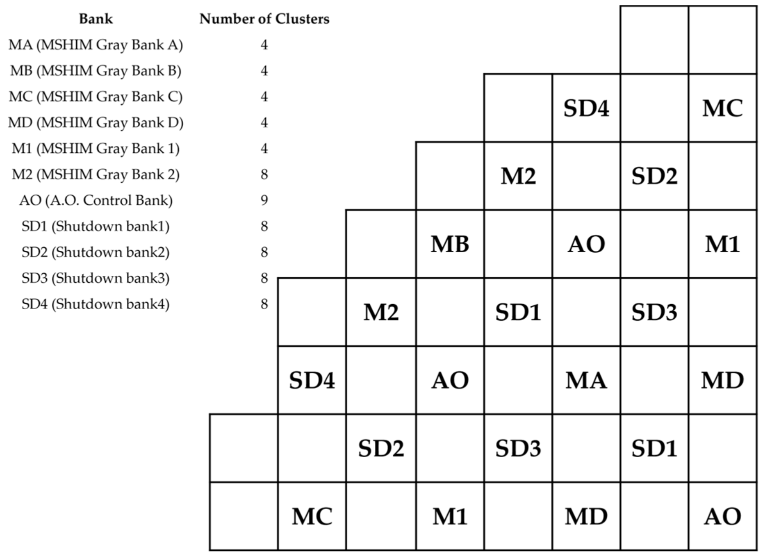

Figure 3. AP1000 core quarter control rod assemblies layout.

2.2. Calculation Methods

This paper investigates the effects of fuel temperature, boron concentration, control rod position, and moderator density variations on AP1000 reactor reactivity. The paper calculates the temperature reactivity coefficients and control rod worth for different influences.

We also studied the variation of effective delayed neutron fraction (β_{eff}) and effective neutron production time (Λ_{eff}) under different conditions. The effects of the core parameter change on the core neutron flux and relative power density distributions are studied comparatively to analyze the state of the AP1000 reactor core under accident conditions.

The study uses the Monte Carlo particle transport program, RMC [27], to create a detailed three-dimensional model of the AP1000 reactor core based on the AP1000 reactor data from Westinghouse [26]. RMC is the physics computational core of the multi-physics, multi-size coupled nuclear energy system numerical analysis platform. RMC uses the ENDF/B-VII.1 database for complex 3D models. In the calculations, the RMC critical card is set to 20,000 particles per iteration and 500 iterations in total, and the initial 100 inactive generations of neutron records are skipped before counting. Due to the incomplete cross-section data of nuclides at different temperatures in the RMC3.5 software, the NJOY2016 software was used to generate the nuclear cross-section data required for the temperature of the study. Figure 4 shows the detailed 3D model of the AP1000 core created by the RMC3.5 software based on AP1000 reactor data provided by Westinghouse [26].

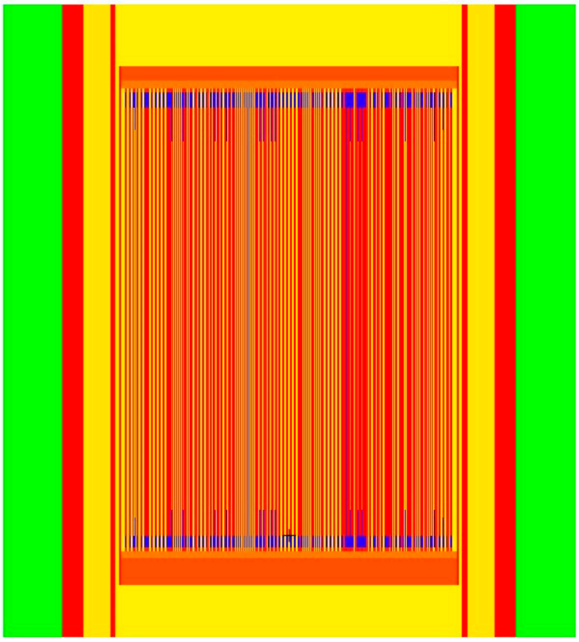

(**a**)

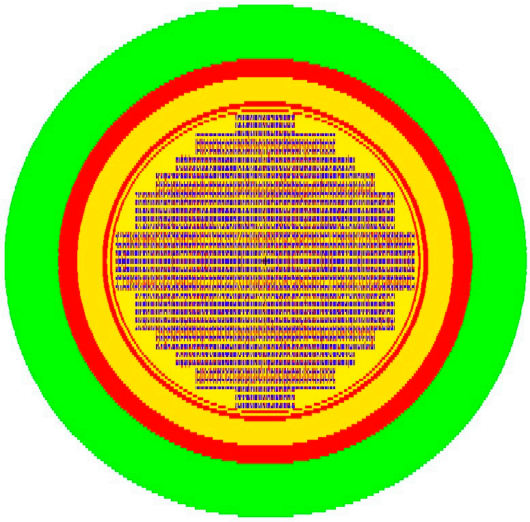

(**b**)

Figure 4. Horizontal (**b**) and vertical cross-section (**a**) of RMC model of AP1000 core.

After the core model was completed, the reliability of the AP1000 core model first needed to be verified. The K_{eff} results calculated by the RMC3.5 software are compared with the values reported by Westinghouse [26]. In the second step, the variation of reactivity was investigated computationally over a wide range of temperatures, limiting values of boron concentration, different densities of moderator, and different positions of the control rods. As shown in Table 2, twenty study conditions are set up according to the three states of AP1000 (CZP, HZP, and HFP). The study conditions include normal and core overheating, boron dilution, and other accidents. In this part of the study, the reactivity of the AP1000 core is evaluated by calculating K_{eff} (including the Doppler Effect, temperature effect, moderator density effect, boron worth, and control rod worth). The above core configurations are symbolized as C1–20.

The main calculations are as follows.

The Doppler effect calculation conditions are from normal operating conditions to core overheating (from 565 K to 732.5 K, 900 K, 1500 K, and 2000 K). Two different sets of calculations were conducted. One is based on soluble boron concentrations of 0 ppm (C1\C2, C1\C3, C1\C4, and C1\C5), and the other is based on soluble boron concentrations of 800 ppm (C9\C10, C9\C11, C9\C12, and C9\C13).

The effect of moderator density is based on the presence or absence of soluble boron, and keeping the fuel temperature constant was explored and calculated (C3\C6, C5\C7, C13, C15, and C11\C14).

The research on soluble boron worth and boron concentration coefficient mainly focuses on the impact of changes in soluble boron concentration on reactivity at different temperatures (C9\C1, C10\C2, C11\C3, C12\C4, and C13\C5).

The study of the control rod worth is determined by the reactivity difference with and without control rod insertion in the core (C9, C10, C17\C11, C13\C19, and C15\C20). For C9 and C10, additional comparisons were made with the control rods fully inserted under the same conditions.

In addition, the effects of temperature variation, coolant density variation, boron concentration reduction, and the position of the control rods in the duct on the neutron flux and relative power density distributions are also investigated.

The neutron flux and relative power density distributions of the fuel assemblies at each operating condition are calculated by using the notation card Type in RMC. The variation of neutron flux and relative power density peak is also studied.

Table 2. Specific parameters for different working conditions.

Core Configurations	Fuel Temperature (K)	Moderator and Structure Temperature (K)	Moderator Density (g/cm^3)	CB (ppm)	Control Rods Position
C1-HZP	565	565	0.7431	0	Remove
C2	732.5	565	0.7431	0	Remove
C3-HFP	900	565	0.7431	0	Remove
C4	1500	565	0.7431	0	Remove
C5	2000	565	0.7431	0	Remove
C6	900	-	0.2	0	Remove
C7	2000	-	0.2	0	Remove
C8	293.6	293.6	1	0	Remove
C9	565	565	0.7431	800	Remove
C10	732.5	565	0.7431	800	Remove
C11	900	565	0.7431	800	Remove
C12	1500	565	0.7431	800	Remove
C13	2000	565	0.7431	800	Remove
C14	900	-	0.2	800	Remove
C15	2000	-	0.2	800	Remove
C16	293.6	293.6	1	800	Remove
C17	900	565	0.7431	800	Insert
C18-CZP	293.6	293.6	0.995	0	Remove
C19	2000	565	0.7431	800	Insert
C20	2000	-	0.2	800	Insert

3. Results and Discussion

As shown in Table 3, to verify the reliability of the RMC modeling, the K_{eff} results of the RMC3.5 software for different core states are compared with the benchmark values provided by Westinghouse [26]. The study examines three distinct operating conditions: when the core is at cold zero power with a boron concentration of 1574 ppm; when the core is at cold zero power with a boron concentration of 1502 ppm; when the core is at hot zero power operating conditions.

Table 3. Comparison of calculated results with Westinghouse benchmarks.

Core States	K_{eff} (RMC Results)	Westinghouse Benchmark	Deviation (%)
C-CZP	1.20469 ± 0.00027	1.205	−0.031
C-CZP (B1574)	0.99472 ± 0.00022	0.99	0.472
C-HZP (B1502)	0.99298 ± 0.00004	0.99	0.298

The statistical uncertainty associated [28] with the RMC critical calculations was identified as the standard deviation (σ), and this is also reflected in Table 3. It is used to indicate the reliability of the cyclic data. According to the comparison of the data in Table 3, the calculated data shows some deviation in the states of CZP and HZP. In the state of C-CZP (B1574ppm), there is a maximum deviation of 0.472% in the calculated data. The reason for the deviation may be that the nuclear database used in this paper is different from the one used in the Westinghouse benchmarking report. The K_{eff} provided in the benchmarking report has only two or three decimal places, which may also contribute to the deviation due to the lack of clarity of the data after the decimal point. Overall, the results of the RMC model calculations compared to the Westinghouse benchmark [26] are within acceptable limits. The reliability of the modeling was demonstrated, and the computational capability of the RMC program was confirmed.

After verifying the reliability of the model, the effects of changes in fuel temperature, moderator density, and boron concentration on reactivity are calculated according to the conditions. The reactivity coefficients, effective delayed neutron fractions, control rod worth, neutron fluxes, and relative power density distributions are further evaluated and calculated in combination with the results of the calculations and the definitions of the safety parameters.

Firstly, the K_{eff} for the AP1000 model calculation study conditions need to be calculated. The K_{eff} and core excess reactivity for different core conditions are shown in Table 4. The study also presents the standard deviation (σ) of the calculated effective multiplication factor (K_{eff}) in Table 4.

Table 4. Effective multiplication factors (K_{eff}) and standard deviation (σ) under different conditions.

Core Configurations	$K_{eff} \pm \sigma$	Excess Reactivity (%)	Core Conditions	$K_{eff} \pm \sigma$	Excess Reactivity (%)
C1-HZP	1.11837 ± 0.00026	10.584	C9	1.02692 ± 0.00026	2.515
C2	1.11373 ± 0.00026	10.212	C10	1.02209 ± 0.00027	2.161
C3-HFP	1.10895 ± 0.00027	9.825	C11	1.01729 ± 0.00026	1.700
C4	1.09563 ± 0.00029	8.728	C12	1.00573 ± 0.00028	0.570
C5	1.08651 ± 0.00025	7.962	C13	0.99772 ± 0.00025	−0.229
C6	0.83258 ± 0.00062	−20.109	C14	0.81317 ± 0.00025	−22.976
C7	0.80471 ± 0.00024	−24.268	C15	0.78680 ± 0.00025	−27.097
C8	1.17463 ± 0.00028	14.867	C16	1.04521 ± 0.00028	4.325
C17	0.89371 ± 0.00028	−11.893	C19	0.87638 ± 0.00028	−14.106
C18-CZP	1.20187 ± 0.00027	16.796	C20	0.66483 ± 0.00023	−50.414

3.1. Reactivity Coefficient

Calculations were performed to evaluate the reactivity changes under different operating conditions. The main components are the Doppler effect, moderator density coefficient (MDC), and soluble boron worth. We have analyzed and calculated the FTC, MDC, and boron worth for accident conditions such as core overheating and boron dilution using RMC3.5 software and NJOY2016 software. The parameters calculated from the study were compared with the limit values in the AP1000 design report provided by Westinghouse benchmarking to assess the safety status of the AP1000 reactor under different conditions.

The reactivity changes caused by different condition changes were calculated using Equation (1).

$$\Delta\rho_i = (K_a - K_b)/(K_a \cdot K_b), \quad (1)$$

where $\Delta\rho_i$ is the variation of reactivity under different study conditions, K_a and K_b are the effective multiplication factors of the core under condition a and condition b, respectively.

The parameters calculated for the study were compared to the limits in the AP1000 design literature provided by the Westinghouse benchmark to evaluate the safety status of the AP1000 reactor under different conditions.

3.1.1. Reactivity Temperature Coefficient

The change in reactivity per unit change in fuel temperature is defined as the fuel temperature coefficient (FTC). This section investigates the calculation of the effect of fuel temperature variation on the reactivity of the core, and the FTC is calculated using Equation (2).

$$\mathrm{FTC} = \Delta\rho_{\mathrm{d}} / \Delta T_{\mathrm{fuel}}, \tag{2}$$

where FTC is the fuel temperature coefficient, $\Delta\rho_{\mathrm{d}}$ is the Doppler effect, and ΔT_{fuel} is the amount of fuel temperature change.

The variation of the K_{eff} with fuel temperature variation is shown in Figure 5. The effect of fuel temperature variation on reactivity in the absence of boron and at a boron concentration of 800 ppm is given in Table 5. The total temperature reactivity variation from cold to hot temperature is given in Table 6. Fuel temperature and moderator density were considered for the study and used to calculate the total temperature reactivity effect.

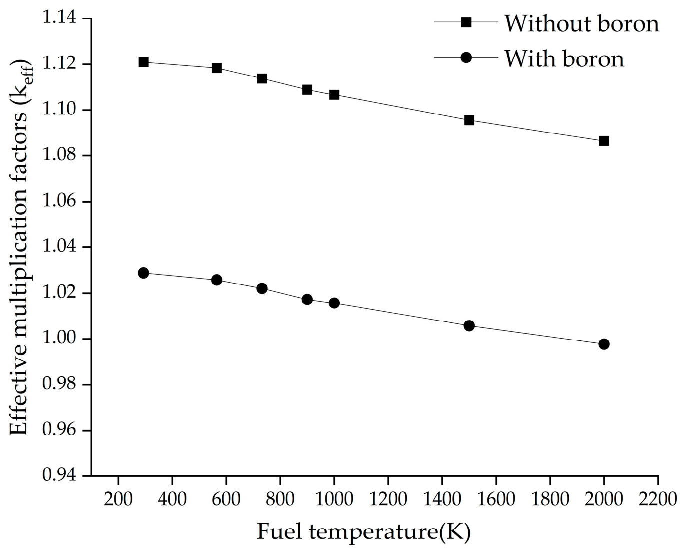

Figure 5. Variation curve of effective multiplication factor (K_{eff}) with fuel temperature.

Table 5. Doppler effect and fuel temperature coefficient.

Research Conditions	Fuel Temperature Variation (ΔK)	Doppler Defect (pcm)	FTC (pcm/K)
C1,C2 (CB = 0 ppm)	167.5	−372.523	−2.224
C1, C3 (CB = 0 ppm)	335	−759.545	−2.267
C1, C4 (CB = 0 ppm)	935	−1855.842	−1.985
C1, C5 (CB = 0 ppm)	1435	−2621.963	−1.827
C9, C10 (CB = 800 ppm)	167.5	−460.173	−2.747
C9, C11 (CB = 800 ppm)	335	−921.817	−2.434
C9, C12 (CB = 800 ppm)	935	−2051.696	−2.081
C9, C13 (CB = 800 ppm)	1435	−2849.952	−1.912

Table 6. Temperature effect.

CB (ppm)	Research Conditions	Temperature Effect (pcm)
0	C8, C1	−4282.655
800	C16, C9	−1704.015

Combining the calculated data in Table 4 and Figure 5, it can be seen that the K_{eff} decreases with increasing fuel temperature. This is due to the increase in fuel temperature, which makes the share of neutrons absorbed by ^{238}U increase. The thermal motion of the ^{238}U nucleus is enhanced with the increase in temperature, and the broadening of the resonance peak of its resonance capture cross-section leads to an increase in the number of neutrons absorbed by resonance, a decrease in the escape resonance capture probability, and a decrease in the number of fission neutrons in the fuel, leading to a decrease in the K_{eff} of the core.

The calculated results show that both reactivity and FTC show negative feedback. As shown in Table 5, the Doppler effect always maintains negative feedback in the studied temperature range (565–2000 K). The FTC results are in the range of −2.434 pcm/K to −1.827 pcm/K for the studied conditions. A negative reactivity coefficient ensures the safe operation of the reactor. In the event of core overheating or fuel temperature rise, a negative temperature coefficient leads to a reduction in reactor power and a gradual reduction in reactor temperature, which ensures the safety of the reactor. The results are within the design limits of −3.5 pcm/K to −1 pcm/K in the Westinghouse [26] report, which demonstrates the inherent stability of the AP1000 core at high temperatures. Table 5 provides a detailed comparison of the fuel temperature coefficients (FTC) for boron-containing and boron-free coolants. The boron-containing coolant exhibits stronger negative feedback for the same temperature change. A coolant with a boron concentration of 800 ppm has a stronger negative effect on fuel temperature than a coolant without boron. This was more pronounced at higher temperature variations (ΔT) and higher temperatures. This indicates that the AP1000 core has a stronger temperature effect after the use of boron-containing coolant. Table 6 shows the results of the temperature effect in the hot zero power (HZP) and cold zero power (CZP) states calculated from the analysis [29].

3.1.2. Moderator Density Coefficient

The moderator density is largely influenced by the moderator temperature. Moderator density decreases with increasing moderator temperature. Here, we mainly study the reactivity change caused by the change in the density of the moderator under the operating condition of continuous overheating of the core, which causes the density of the moderator to decrease.

The change in reactivity due to a change in temperature per unit of moderator is described as the moderator temperature coefficient (MTC). The moderator density coefficient is calculated by Equation (3).

$$MDC = \Delta\rho_{md}/\Delta P_{md}, \tag{3}$$

where MDC is the moderator density coefficient, $\Delta\rho_{md}$ is the moderator density effect, and ΔP_{md} is the amount of moderator density change.

Table 7 gives the effect of large changes in the density of the moderator on the reactivity of the core, and Figure 6 shows the curve of the K_{eff} with the density of the moderator.

Table 7. Density coefficients and reactivity induced by moderators.

Research Conditions	Effect of Decreasing Moderator Density (pcm)	MDC (pcm/g/cm^3)
C3, C6 (CB = 0 ppm)	−29,933.187	−55,115.424
C5, C7 (CB = 0 ppm)	−32,230.561	−59,345.536
C13, C15 (CB = 800 ppm)	−26,868.581	−49,472.622
C11, C14 (CB = 800 ppm)	−24,675.129	−45,433.859

From the results of the curve changes in Table 4 and Figure 6, it can be seen that decreasing the density of the moderator makes the K_{eff} decrease. This is due to the decrease in the density of the moderator, which makes the moderator slow the ability to increase the resonance absorption. The increase in the temperature of the moderator hardens the neutron energy spectrum and causes an increase in the resonance absorption of the low-energy part of elements such as ^{238}U, causing a negative reactivity effect.

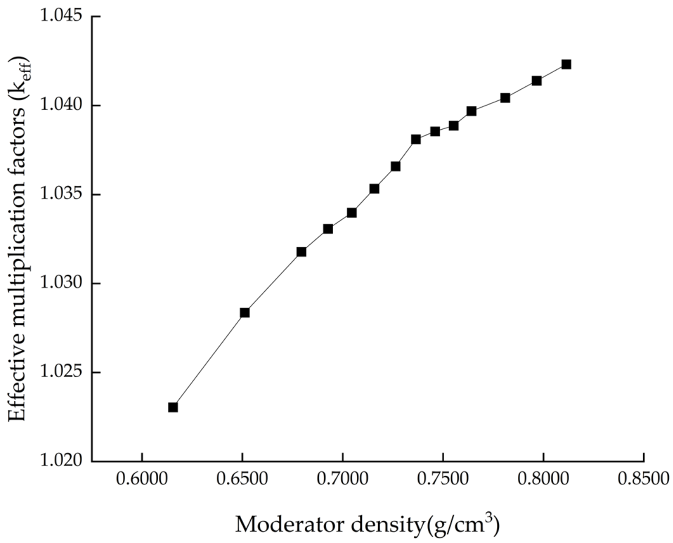

Figure 6. The curve of effective multiplication facto (K_{eff}) with the density of moderator.

In addition, it is clear from the calculations in Table 7 that the absence of soluble boron makes the negative reactivity feedback effect stronger. The moderator density coefficients are consistently negative, facilitating self-regulation of reactor power. The calculated data in Table 7 illustrates the inherent safety of the AP1000 core design. It also demonstrates the rationalization of the AP1000 design under unanticipated operating conditions of core overheating and reduced moderator density.

3.1.3. Boron Concentration Coefficient

The soluble boron worth is the change in reactivity of the core caused by a change in unit boron concentration in the coolant.

The boron concentration factor is calculated using Equation (4).

$$BCC = \Delta\rho_b/\Delta C_b, \tag{4}$$

where BCC is the boron concentration coefficient, $\Delta\rho_b$ is the soluble boron value, and ΔC_b is the amount of boron concentration change.

The effect of soluble boron concentration variation on core reactivity at different temperatures is given in Table 8. The effect of boron concentration on K_{eff} is shown in Figure 7. As can be seen from Table 4 and Figure 7, K_{eff} decreases as the boron concentration increases. This is because the addition of boric acid solution to the coolant is a chemically compensated control for controlling the reactivity of the core, and the higher the concentration of soluble boron, the higher the ability to absorb neutrons and, thus, the lower K_{eff}.

Table 8. Soluble boron worth and boron concentration coefficient.

Fuel Temperature (K)	Research Conditions	Soluble Boron Worth (%)	BCC (pcm/ppm)
565	C9, C1-HZP	−7.963	−9.953
732.5	C10, C2	−8.050	−10.063
900	C11, C3-HFP	−8.125	−10.156
1500	C12, C4	−8.159	−10.198
2000	C13, C5	−8.191	−10.238

As shown in Table 8, the change in reactivity of the core is negative with increasing concentration of boric acid, the boron concentration factor is also negative, and the boron concentration factor decreases with increasing temperature in the fuel zone. Comparing the studied boron concentration factors for different conditions with the design limits in the

Westinghouse report (which range from −13.5 pcm/ppm to −5.0 pcm/ppm) shows that the AP1000 core is in a safe condition under accident conditions such as core overheating.

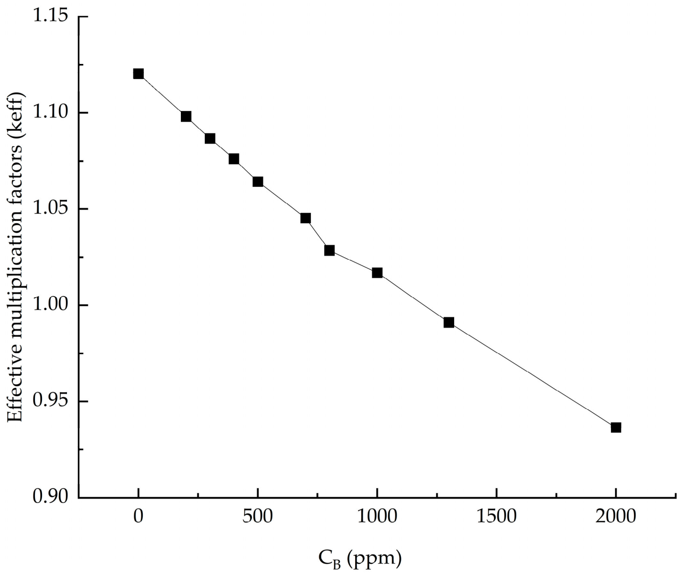

Figure 7. The curve of effective multiplication factor (K_{eff}) with the boron concentration.

From the results of the study, it can be seen that the FTC, BCC, and MDC of the AP1000 are still negative under the conditions of an accident in the core. The positive reactivity coefficients cause an increase in core power. Without introducing external reactivity control, it may lead to a core meltdown. The results show that the AP1000 reactor core state maintains negative feedback at high temperatures of 2000 K. The calculated values of FTC, BCC, and MDC are within the limits of the AP1000, which proves that the AP1000 reactor has sufficient safety margins.

3.1.4. Control Rods Worth

The CRW is defined as the amount of change in reactivity with the control rod present until the control rod is fully proposed.

The control rod worth is calculated by Equation (5).

$$CRW = 1/K_r - 1/K_e, \tag{5}$$

where CRW is the control rod's worth, K_r is the effective multiplication factor for the initial state without control rods, and K_e is the effective multiplication factor for all inserted states of control rods.

The calculation in Table 9 shows the CRW at different temperatures for a boron concentration of 800 ppm. Comparative conditions are provided for C9 and C10 (with the control rods fully inserted under the same conditions).

Table 9. Effect of control rods position on reactivity and control rods worth.

Research Conditions	Fuel Temperature (K)	CRW (pcm)
C9, Supplement	565	14,593.483
C10, Supplement	732.5	14,417.381
C17, C11	900	13,592.733
C13, C19	2000	13,877.232
C15, C20 (low density)	2000	23,317.289

The effect of temperature on the CRW was mainly investigated. From the data in Table 9, it can be seen that the CRW decreases with increasing temperature when the temperature in the fuel zone increases from 565 K to 900 K. When the temperature continues to increase and the core overheats, the CRW increases. The reason is that, under accident conditions, the moderator density decreases due to the continuous high temperature of the core, which leads to a significant increase in the CRW. It also indicates that the control rods are worth enough to shut down the reactor in case of an emergent situation, which guarantees the safety of the reactor to some extent.

3.2. Effective Delayed Neutron Fraction and Neutron Generation Time

The effective delayed neutron fraction (β_{eff}) [19] and the effective neutron generation time (Λ_{eff}) [19] are used as essential reactor parameters, and studying them can provide deeper insight into the core performance. The delayed neutron fraction is the total fraction of delayed neutrons in the total fission neutrons.

The β_{eff} is calculated using Equation (6), and the Λ_{eff} is calculated using Equation (7).

$$\beta_{eff} = \left(K_{eff} - K_p\right)/K_{eff}, \tag{6}$$

$$\Lambda_{eff} = l_p/K_{eff}, \tag{7}$$

In Equation (6), β_{eff} is the effective delayed neutron fraction, K_{eff} is the final result of the effective multiplication factor of the RMC3.5 software cycling run, and K_p is the multiplication factor of the prompt neutrons cycled after using the ResponseMT card.

In Equation (7), Λ_{eff} is the effective neutron generation time, and l_p is the neutron lifetime.

The results of the β_{eff} calculation are shown in Table 10. Table 10 shows the variation of β_{eff} in different core states. From the data in Table 10, it can be seen that β_{eff} decreases when the temperature is increased from 565 K to 1500 K, regardless of whether the coolant contains boron or not. This indicates that the increase in temperature has a certain effect on the content of delayed neutrons. However, when the core is overheated and the fuel temperature reaches 2000 K, the β_{eff} increases.

Table 10. Effective delayed neutron fraction at different operating conditions.

Core Configurations	Fuel Temperature (K)	$K_{eff} \pm \sigma$	$K_p \pm \sigma$	β_{eff}
C1-HZP	565	1.11837 ± 0.00026	1.10953 ± 0.00026	0.00812
C2	732.5	1.11373 ± 0.00026	1.10509 ± 0.00027	0.00789
C3-HFP	900	1.10895 ± 0.00027	1.10143 ± 0.00028	0.00688
C4	1500	1.09563 ± 0.00029	1.08812 ± 0.00026	0.00684
C5	2000	1.08651 ± 0.00025	1.07771 ± 0.00024	0.00818
C6 (low density)	900	0.83258 ± 0.00062	0.82524 ± 0.00024	0.00878
C7 (Core overheating, low density)	2000	0.80471 ± 0.00024	0.79871 ± 0.00026	0.00746
C9	565	1.02692 ± 0.00026	1.01807 ± 0.00026	0.00862
C10	732.5	1.02209 ± 0.00027	1.01472 ± 0.00026	0.00721
C11	900	1.01729 ± 0.00026	1.01078 ± 0.00027	0.00640
C12	1500	1.00573 ± 0.00028	0.99920 ± 0.00029	0.00635
C13	2000	0.99772 ± 0.00025	0.99024 ± 0.00024	0.00750
C14 (low density)	900	0.81317 ± 0.00025	0.80658 ± 0.00024	0.00810
C15 (Core overheating, low density)	2000	0.78680 ± 0.00025	0.78103 ± 0.00023	0.00733

Since recoil plays a major role in the production of delayed neutron precursor nuclei [30] under low-temperature operating conditions, recoil is not sensitive to temperature. At high temperatures, the generation of delayed neutron pioneers is mainly affected by thermal diffusion. Thus, it is more affected by temperature. At high temperatures, the delayed neutron fraction decreases and the prompt neutron content is higher. To some extent, this suggests that core overheating may lead to uncontrolled reactors.

The Λ_{eff} and standard deviations simulated by the software under different conditions are shown in Table 11. The neutron lifetime is calculated by Equation (7). From Table 11, it can be concluded that the prompt neutron lifetime is larger without soluble boron compared to the results with soluble boron. Comparing C1 to C4 and C9, C12, it can be seen that the neutron lifetime decreases as the fuel temperature increases up to 1500 K. In contrast, a small increase in the neutron lifetime is observed at 2000 K. This is due to the delayed effect that causes the neutron lifetime to decrease. Thus, the change in the share of delayed neutrons affects the neutron lifetime.

Table 11. Neutron lifetime and neutron generation time.

Core Configurations	Prompt Neutron Lifetime, l_{eff} (s)	Standard Deviation (σ)	Neutron Generation Time, Λ_{eff} (μs)
C1-HZP	2.59780×10^{-5}	4.36310×10^{-8}	23.22845
C2	2.58140×10^{-5}	3.45750×10^{-8}	23.17797
C3-HFP	2.55950×10^{-5}	3.20930×10^{-8}	23.08039
C4	2.52870×10^{-5}	4.55570×10^{-8}	23.07987
C5	2.53930×10^{-5}	3.26640×10^{-8}	23.37116
C9	1.99890×10^{-5}	1.82850×10^{-8}	19.46500
C10	1.98740×10^{-5}	1.42350×10^{-8}	19.44447
C11	1.97080×10^{-5}	1.96080×10^{-8}	19.37304
C12	1.94790×10^{-5}	1.97810×10^{-8}	19.36802
C13	1.93750×10^{-5}	2.01410×10^{-8}	19.41900

3.3. Neutron Flux and Relative Power Density Distribution

In this section, the effects of different conditions on the distribution of neutron flux and relative power density in the core were studied.

As shown in Figures 8 and 9, the two figures show the neutron flux and relative power distribution for the hot full power (HZP) condition with coolant condition without soluble boron (C3-HFP) and coolant condition with 800 ppm boron concentration (C11), respectively. The distribution of neutron flux and relative power density with and without soluble boron, core overheating, and low moderator (C7, C15) density is shown in Figures 10 and 11.

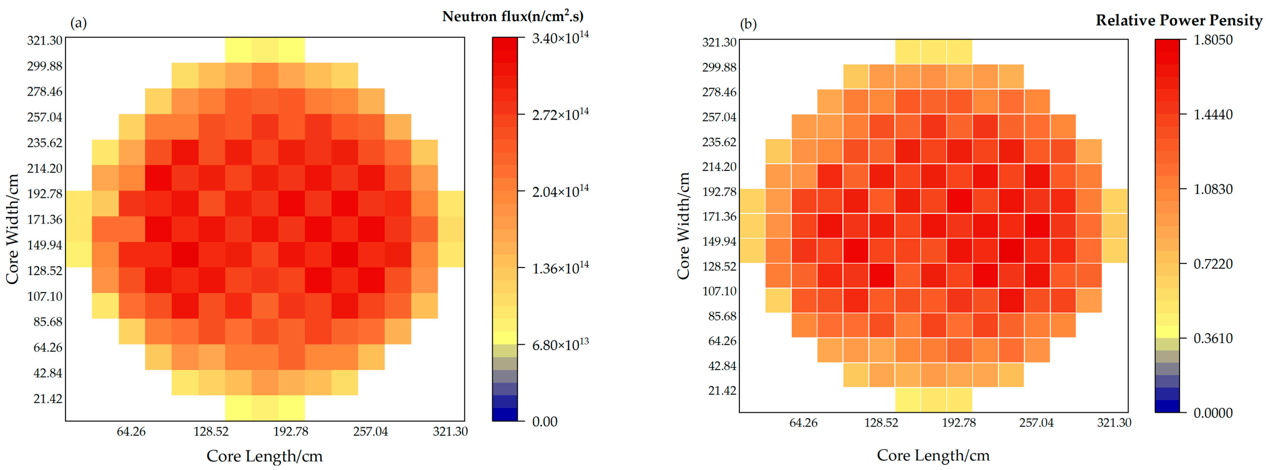

Figure 8. Neutron flux (**a**) and relative power density (**b**) of AP1000 core without soluble boron and control rod HZP condition (C3).

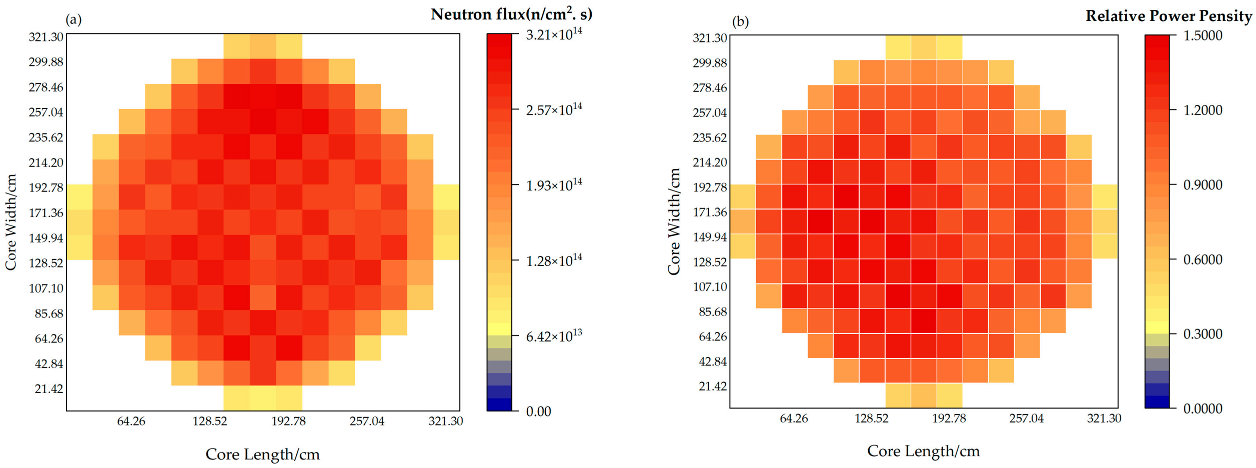

Figure 9. Neutron flux (**a**) and relative power density (**b**) in AP1000 core with soluble boron and without control rods (C11).

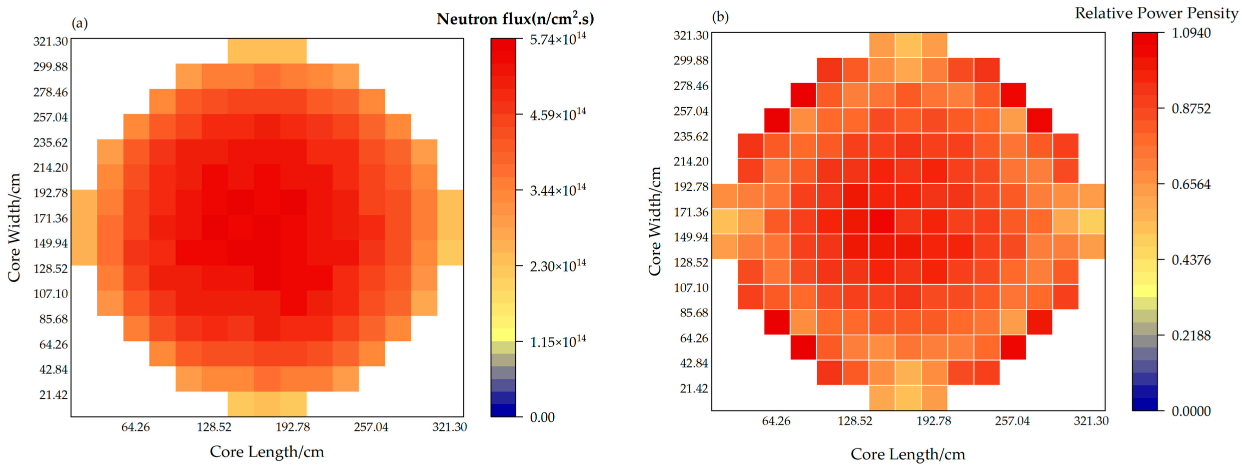

Figure 10. Neutron flux (**a**) and relative power density (**b**) of AP1000 core without soluble boron and control rods and under overheated core (low density) conditions (C7).

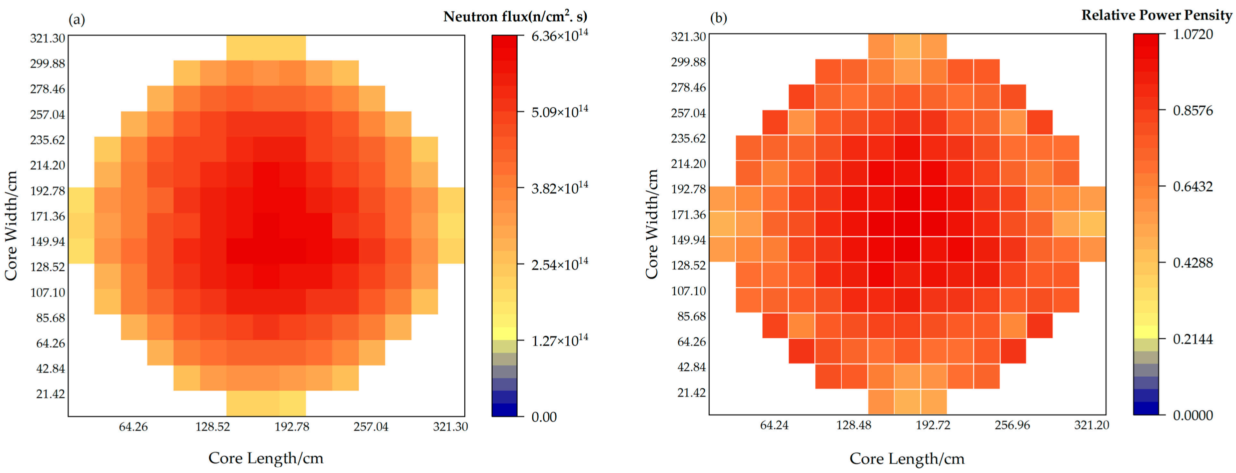

Figure 11. Neutron flux (**a**) and relative power density (**b**) of AP1000 core with soluble boron without control rods and overheated core (C15).

In addition, the control rod position effects on the neutron flux and power density distributions at HZP temperature (C17), core overheating (C19), and moderator density reduction (C20) are also investigated, and the results are shown in Figures 12–14, respectively. The comparative study with the sudden core overheating condition (C13) is shown in Figure 15.

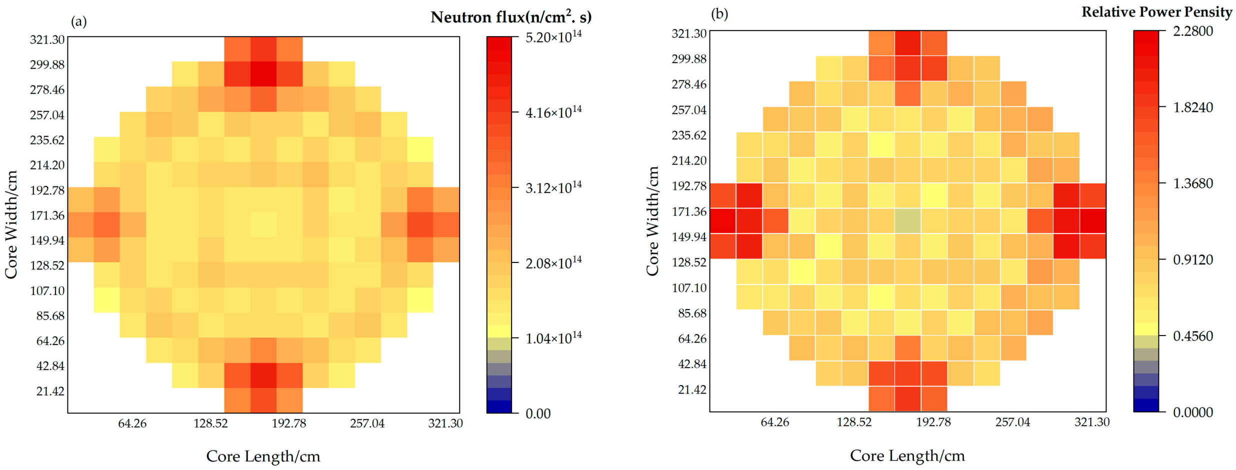

Figure 12. Neutron flux (**a**) and relative power density (**b**) of control rods fully inserted into AP1000 core under HZP condition with soluble boron (C17).

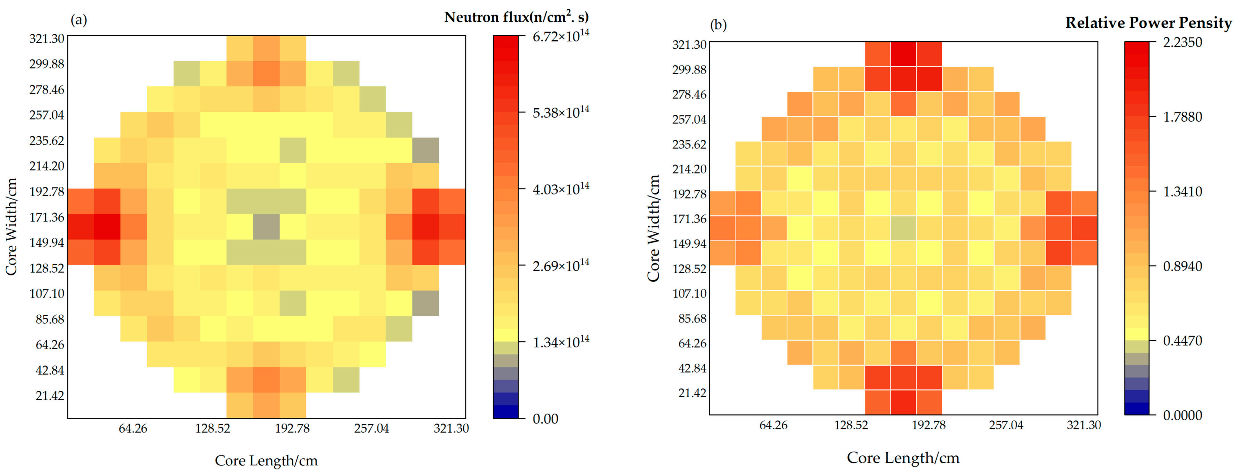

Figure 13. Neutron flux (**a**) and relative power density (**b**) of AP1000 core with soluble boron and full insertion of control rods and overheated core (C19).

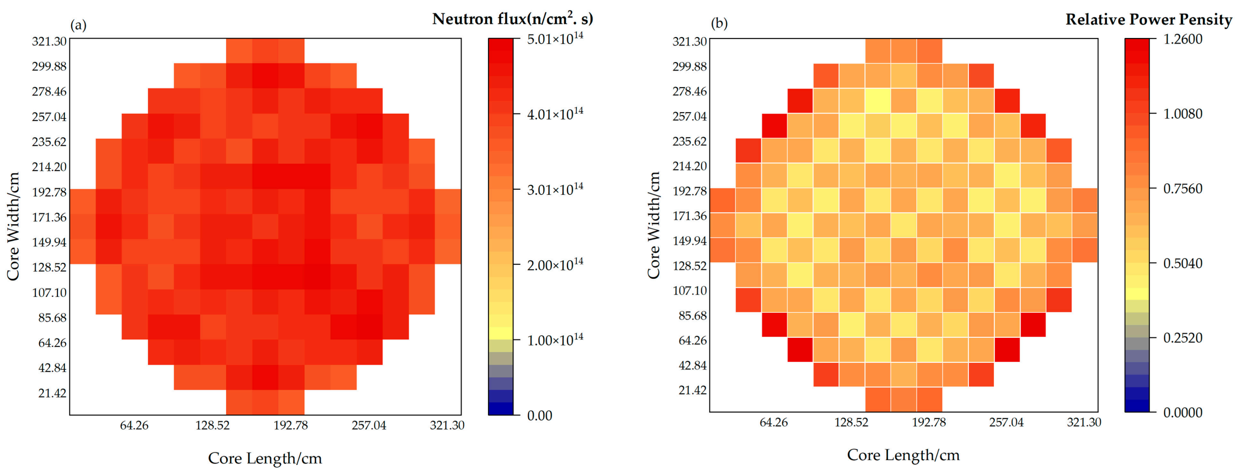

Figure 14. Neutron flux (**a**) and relative power density (**b**) in AP1000 core with soluble boron and fully inserted control rods and overheated core (low density) (C20).

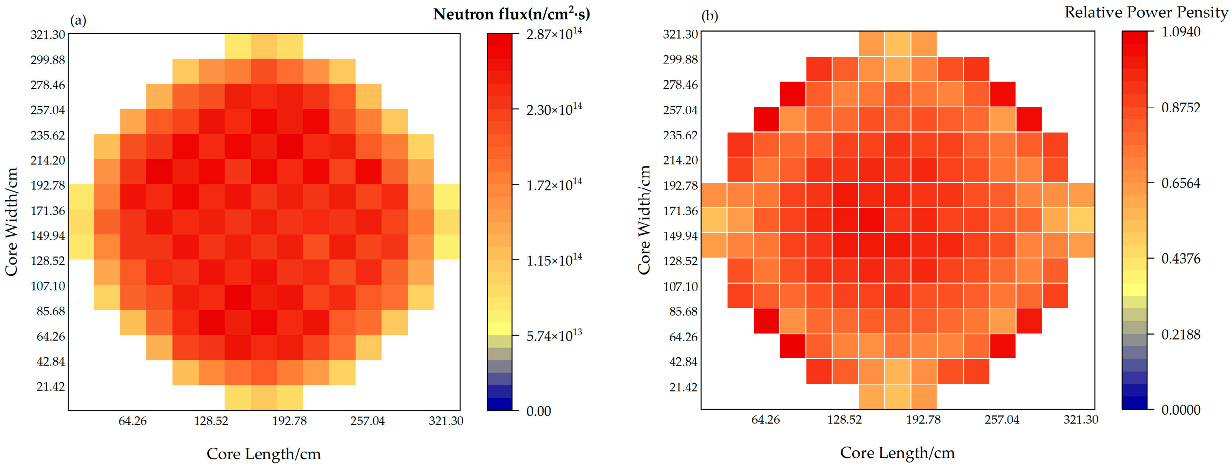

Figure 15. Neutron flux (**a**) and relative power density (**b**) of AP1000 core with soluble boron control without control rods and under overheated core conditions (C13).

The impact of boron concentration on the flux is shown in Figures 8 and 9. In the HZP condition, the addition of boron makes the neutron flux distribution more uniform. The maximum neutron flux peak and power density peak in the condition with boron (C11) are lower than the flux values in the condition without boron (C3-HFP). This indicates that the chemical control of AP1000 can interact with the fuel zone to reduce the flux peak and make the flux distribution more uniform in the radial direction. Similarly, the effect of boron concentration on flux is also reflected in the accident conditions (C7, C15), as shown in Figures 10 and 11.

The effect of a sudden temperature increase on neutron flux is shown in Figure 15. Since the fuel temperature effect is transient, the peak power density increases under the core overheating (C13) condition. Figures 8–11 show the neutron flux and power density with boron (C11 and C15) and without boron (C3-HFP and C7), respectively. The figures show that the core overheats and the neutron flux increases, and the reactor power is automatically regulated due to the temperature coefficient of the core overheating showing negative feedback, and the power density decreases as the reactivity decreases.

The effect of the CRW on the flux distribution is analyzed by comparing Figures 9 and 12 (C11 and C17 on the HZP condition) at a fuel temperature of 900 K and Figures 13 and 15 (C13 and C19 on the core overheating condition) at a fuel temperature of 2000 K. It can be seen that the insertion of the control rods leads to a large change in the peak position of the neutron flux energy spectrum and distortions in both the neutron flux distribution and the relative power density distribution. In addition, the peak neutron flux and power density when the control bar is fully inserted are higher than the peak neutron flux and power density when the control bar is fully proposed.

As can be seen from Figures 12–14 (C17, C19, and C20), when the control rods are fully inserted, the effect of the change in moderator density on the flux is greater than the effect produced by the change in fuel temperature. The overheating of the core and the decrease in the moderator density incline the neutron flux distribution toward the center of the core and lower neutron fluxes in the peripheral fuel assemblies. In addition, the decrease in moderator density results in a lower peak power density.

The above analysis shows that the neutron flux and power density distributions are affected by fuel temperature, moderator density, and control rod position. The peak neutron flux and peak power density increased with temperature, with the decrease in boron concentration, and the insertion of the control rods.

4. Conclusions

In this paper, the changes in safety parameters such as reactivity coefficient, CRW, β_{eff}, neutron generation time, and neutron flux of AP1000 reactor under normal and accident conditions are investigated. The AP1000 core is modeled and simulated using RMC to calculate changes in temperature and moderator density limits, as well as the presence or absence of soluble boron. We also study changes in core reactivity under accident conditions, such as core overheating. The conclusions are as follows.

The AP1000 reactor still has negative reactivity coefficients, such as FTC under core overheating and boron dilution accident conditions. This indicates that the AP1000 is still relatively safe under the accident conditions studied in this paper. In addition, the FTC has stronger negative feedback for the same conditions of temperature variation containing boron, indicating the ability of boron to modulate the AP1000 reactor.

The K_{eff} decreases with increasing boron concentration. The BCC decreases with increasing temperature. This illustrates the role of boron in modulating reactivity. The CRW decreases as temperature increases and increases further when the core overheats. This indicates that the control rods are designed to be sufficient to shut down the reactor in case of an emergency.

The β_{eff} gradually decreases with the increase in temperature from 565 K to 1500 K. However, when the core overheats and the fuel temperature reaches 2000 K, the β_{eff} increases. This change reflects the different generation mechanisms of the delayed neutron nuclei at high temperatures compared to low-temperature nuclei. In addition, the delayed neutron fraction is influenced by the moderator density and soluble boron concentration.

The neutron flux and power density distributions are affected by the fuel and moderator temperatures and control rod positions. The peak neutron flux and power density increased with temperature, decrease in boron concentration, and insertion of the control rods. However, the insertion of control rods causes distortions in both neutron flux distribution and power density distribution. Overheating of the core and a reduction in the moderator density make the neutron flux distribution incline toward the center of the core and lower neutron flux in the peripheral fuel assemblies. In addition, the decrease in moderator density reduces the peak power density.

Author Contributions: Conceptualization, X.N.; methodology, X.N.; software, X.N. and J.L.; validation, X.N., J.L., Z.D., J.W. and W.Z.; formal analysis, X.N.; resources, X.N. and J.L.; data curation, X.N.; writing—original draft preparation, X.N.; writing—review and editing, J.L., Z.D., J.W. and W.Z.; supervision, J.L., Z.D., J.W. and W.Z. All authors have read and agreed to the published version of the manuscript.

Funding: This research received no external funding.

Data Availability Statement: Data are contained within the article.

Acknowledgments: We thank the School of Energy and Mechanical Engineering, Shanghai University of Electric Power, for supporting this study.

Conflicts of Interest: The authors declare no conflict of interest.

Nomenclature

LWR	Light Water Reactors	HWR	Heavy Water Reactors
K_{eff}	effective multiplication factor	BCC	boron concentration coefficient
HFP	hot full power	CRW	control rod worth
HZP	hot zero power	RTC	reactivity temperature coefficient
CZP	cold zero power	β_{eff}	effective delayed neutron fraction
FTC	fuel temperature coefficient	Λ_{eff}	effective neutron generation time
MDC	moderator density coefficient	σ	standard deviation

Appendix A

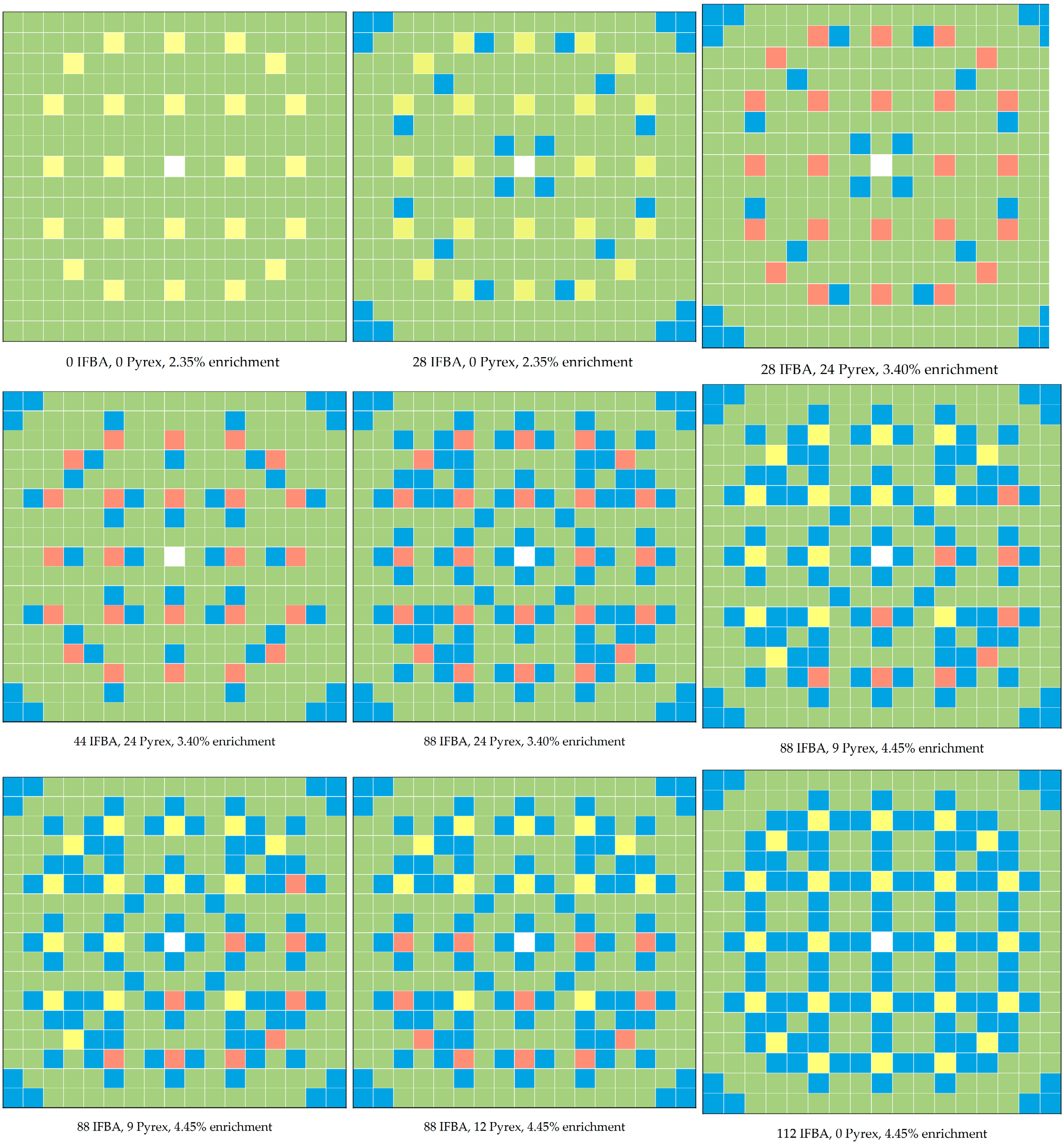

Figure A1. The 9 types of fuel assembly rod bundle distribution.

References

1. Wu, S.; Ma, X.; Liu, J.; Wan, J.; Wang, P.; Su, G.H. A load following control strategy for Chinese Modular High-Temperature Gas-Cooled Reactor HTR-PM. *Energy* **2023**, *263*, 125459. [CrossRef]
2. Oettingen, M.; Cetnar, J. Comparative analysis between measured and calculated concentrations of major actinides using destructive assay data from ohi-2 pwr. *Nukleonika* **2015**, *60*, 571–580. [CrossRef]
3. Oettingen, M.; Cetnar, J. Validation of gadolinium burnout using pwr benchmark specification. *Nucl. Eng. Des.* **2014**, *273*, 359–366. [CrossRef]
4. Jakub, S.; Dabrowski Mariusz, P.; Konrad, C. Negative temperature coefficients of reactivity for metallic fuel Dual Fluid Reactor. *Prog. Nucl. Energy* **2022**, *146*, 104126. [CrossRef]

5. Betzler, B.R.; Ade, B.J.; Wysocki, A.J.; Terrani, K.A. Transformational Challenge Reactor preconceptual core design studies. *Nucl. Eng. Des.* **2020**, *367*, 110781. [CrossRef]
6. Pinem, S.; Sembiring, T.M.; Tukiran; Deswandri; Sunaryo, G.R. Reactivity Coefficient Calculation for AP1000 Reactor Using the NODAL3 Code. *J. Phys. Conf. Ser.* **2018**, *962*, 012057. [CrossRef]
7. de Stefani, G.L.; Moreira, J.M.L.; Maiorino, J.R.; Rossi, P.C.R. Detailed neutronic calculations of the AP1000 reactor core with the Serpent code. *Prog. Nucl. Energy* **2019**, *116*, 95–107. [CrossRef]
8. Thilagam, L.; Mohapatra, D. *Comparison of Physics Characteristics of Pressurized Water Reactor Type Advanced Light Water Reactors*; Springer: Singapore, 2020. [CrossRef]
9. Dobuchi, N.; Takeda, S.; Kitada, T. Study on the relation between Doppler reactivity coefficient and resonance integrals of Thorium and Uranium in PWR fuels. *Ann. Nucl. Energy* **2016**, *90*, 191–194. [CrossRef]
10. Kim, K.-O.; Jo, D. Analysis of Doppler coefficients for typical PWR UO_2 and MTR U_3Si_2 -Al fuels using ENDF/B-VI and VII. *Ann. Nucl. Energy* **2015**, *85*, 1024–1028. [CrossRef]
11. Madi, R. Analysis of Doppler Reactivity Coefficient on the Typical Pwr-1000 Reactor with MOX Fuel. *KnE Energy* **2016**, 1. [CrossRef]
12. Yari, M.; Lashkari, A.; Masoudi, S.F.; Hosseinipanah, M. Three-dimensional analysis of temperature effect on control rod worth in TRR. *Nucl. Eng. Technol.* **2018**, *50*, 1266–1276. [CrossRef]
13. Rahgoshay, M.; Noori-Kalkhoran, O. Calculation of control rod worth and temperature reactivity coefficient of fuel and coolant with burn-up changes for VVRS-2MWth nuclear reactor. *Nucl. Eng. Des.* **2013**, *256*, 322–331. [CrossRef]
14. Mazrou, H.; Lababsa, D.; Mokhtari, O. Assessment of the safety impact caused by the variations of the critical position of control rods and by the presence of an in-core flux trap on the power peaking factors in an MTR-type research reactor. *Nucl. Eng. Des.* **2023**, *414*, 112553. [CrossRef]
15. Vrban, B.; Lüley, J.; Farkas, G.; Haščík, J.; Hinca, R.; Petriska, M.; Slugeň, V.; Šimko, J. Temperature coefficients calculation for the first fuel loading of NPP Mochovce 3–4. *Ann. Nucl. Energy* **2014**, *63*, 646–652. [CrossRef]
16. Olatubosun, S.A.; Ayodeji, A.; Amidu, M.A. Safety assessment of AP1000: Common transients, analysis codes, and research gaps. *Nucl. Eng. Des.* **2021**, *375*, 111100. [CrossRef]
17. Winfried, Z.; Nadine, B.; Alexander, A.; Kiril, V. Sensitivities of delayed neutron fractions in the framework of SCALE 6.2. *Ann. Nucl. Energy* **2021**, *153*, 108068.
18. Kodeli, I.A. Sensitivity and uncertainty in the effective delayed neutron fraction (βeff). *Nucl. Instrum. Methods Phys. Res. A* **2013**, *715*, 70–78. [CrossRef]
19. Yamamoto, T.; Sakamoto, H. Monte Carlo sensitivity analysis method for the effective delayed neutron fraction with the differential operator sampling method. *Ann. Nucl. Energy* **2020**, *140*, 107108. [CrossRef]
20. Sembiring, T.; Susilo, J.; Pinem, S. Evaluation of the AP1000 delayed neutron parameters using MCNP6. *J. Phys. Conf. Ser.* **2018**, *962*, 012030. [CrossRef]
21. Westinghouse. *2011 Westinghouse AP1000 Design Control Document Rev. 19. Section 4.3—Reactor, Nuclear Design*; Westinghouse Electirc Company LLC: Cranberry Township, PA, USA, 2011.
22. Franceschini, F.; Godfrey, A.; Kulesza, J.; Oelrich, R.; Stand, W.V.T. *Zero Power Physics Test Simulations for the AP1000®PWR*; No. CASL-U-2014-0012-000; Westinghouse: Pittsburgh, PA, USA, 2014.
23. Wagner, J.C.; Parks, C.V. *Parametric Study of the Effect of Burnable Poison Rods for PWR Burnup Credit*; Office of Scientific & Technical Information Technical Reports; Oak Ridge National Lab (ORNL): Oak Ridge, TN, USA, 2001. [CrossRef]
24. Selim, H.K.; Amin, E.H.; Roushdy, H.E. Rod ejection accident analysis for AP1000 with MOX/UOX mixed core loading. *Ann. Nucl. Energy* **2017**, *109*, 385–395. [CrossRef]
25. Liu, B.; Jia, R.; Han, R.; Lyu, X.; Han, J.; Li, W. Minor actinide transmutation characteristics in AP1000. *Ann. Nucl. Energy* **2018**, *115*, 116–125. [CrossRef]
26. Westinghouse. *2007 Westinghouse AP1000 Design Control Document Rev. 14, Tier 2. Chapter 14, Reactor Section 4.3, Nuclear Design*; ML071580897; Westinghouse Electirc Company LLC: Cranberry Township, PA, USA, 2007.
27. Wang, K.; Li, Z.; She, D.; Liang, J.; Xu, Q.; Qiu, Y.; Yu, J.; Sun, J.; Fan, X.; Yu, G. RMC–A Monte Carlo code for reactor core analysis. *Ann. Nucl. Energy* **2015**, *82*, 121–129. [CrossRef]
28. Dawahra, S.; Khattab, K.; Saba, G. Reactivity temperature coefficients for the HEU and LEU fuel of the MNSR reactor. *Prog. Nucl. Energy* **2016**, *88*, 28–32. [CrossRef]
29. Porhemmat, M.; Hadad, K.; Faghihi, F. PARCS cross-section library generator; part one: Development and verification. *Prog. Nucl. Energy* **2015**, *78*, 155–162. [CrossRef]
30. Qiu, C.; Duan, T.; Liu, Y. Transient simulation and analysis for delayed neutron detection system of China experimental fast reactor. *At. Energy Sci. Technol.* **2009**, *43*, 817–822.